

## CFD SIMULATIONS OF FLOW, HEAT AND MASS TRANSFER IN THIN-FILM EVAPORATOR

Andrzej Kolek, Janusz Dziak and Lechoslaw Krolkowski

Wroclaw University of Technology, Norwida 4/6 Street, Wroclaw 50-373, Poland

andrzej.kolek@pwr.wroc.pl, janusz.dziak@pwr.wroc.pl, lechoslaw.krolkowski@pwr.wroc.pl

### Abstract

Mathematical model of the process that takes place during liquid solution evaporation in the vertical thin-film evaporator of static type was developed. The model consists of differential equations of flow, heat and mass transfer as well as boundary conditions. The model was applied for CFD simulations of water-propylene glycol solutions evaporation under reduced pressure. Axial symmetry approach was adopted. Two-dimensional distributions of water concentrations, temperature, pressure and velocities of liquid and gas were obtained.

**Keywords:** evaporation, thin-film flow, CFD simulation.

### 1. Introduction

Vertical thin-layer evaporators are characterized by small pressure drop and short residence time of the phases in the apparatus, which means also that there is short contact time of the liquid with hot surface of the evaporator wall. These features of the evaporators cause that they are applied in industry for the concentration of heat sensitive liquid solutions especially with high viscosity. Because of low value of pressure drop during gas flow inside the evaporator the boiling temperature of liquid, which is evaporated, depends only on its composition and does not depend on liquid position in the evaporator, which is of great importance in case of evaporation at low pressure. The purpose of this work was performing mathematical simulation of simultaneous processes of momentum, heat and mass transport during surface vaporization of liquid solution in the thin-layer evaporator. The rules of computational fluid dynamics<sup>1</sup> (CFD) were applied in calculations. The simulations help in understanding, why experimental results of two-component liquid solutions distillation in the thin-layer evaporator often differ from the results got theoretically<sup>2</sup>. Theoretical results were obtained applying theory proposed by Billet<sup>3</sup>, which is commonly used in thin-layer evaporator designing practice.

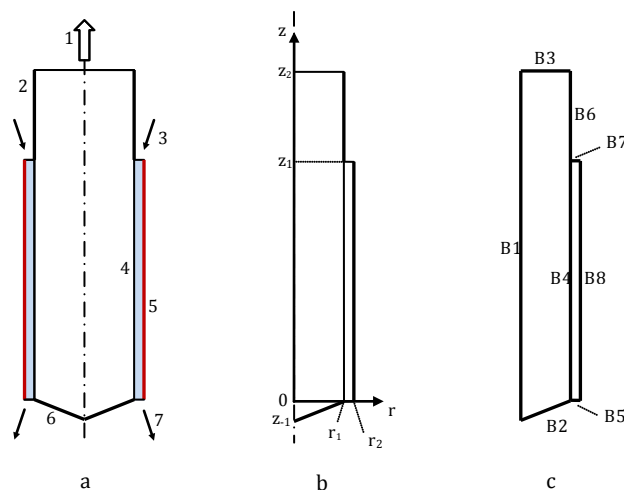


**Figure 1.** a) Object-sketch of the static thin-layer evaporator.

1 – vapor discharge, 2 – thermal insulated wall, 3 – liquid inlet, 4 – interface, 5 – heated wall, 6 – bottom, 7 – liquid discharge.

b) Cylindrical coordinate system arrangement.

$r_1$  – interface radius,  $r_2$  – inner radius of the evaporator,

$z_1$  – liquid layer height,  $z_2$  – gas layer height (without conical bottom).

c) Arrangement and numbering of boundary files.

## 2. Problem statement

The evaporator is constituted by vertical cylinder opened from above and closed at its lower end by conical bottom (Fig.1). At the height of  $z_1$  the multi-component liquid solution is involved, which flows down along the heated surface and evaporates at the same time. The liquid leaves the evaporator at the height  $z_0$ . The generated vapor is discharged from the apparatus at the height  $z_2$ . The ratio of the liquid layer thickness to its height is much lower in reality than one can conclude from the figure. When cylindrical coordinate system is chosen (taking into account axial symmetry of the evaporator), one obtains two-dimensional problem of liquid and gas flow, heat and mass transport and phase transition. The boundary of the flow domain was divided into eight parts: boundary on the axis of symmetry (B1), closed thermal insulated boundaries (B2,B6), closed boundary with fixed temperature (B8), open boundaries: liquid inflow (B7), liquid outflow (B5), gas outflow (B3) and interior boundary (B4), which constitutes gas-liquid interface. Steady state conditions of the evaporator work, with laminar flow of both phases are exclusively considered in this paper.

## 3. Governing equations and boundary conditions

The continuity equation reads :

$$\nabla \cdot (\rho \mathbf{u}) = 0. \quad (1)$$

The momentum equation (Navier-Stokes) is written as

$$\rho \mathbf{u} \cdot \nabla \mathbf{u} = \nabla \cdot \mathfrak{S} - \rho \mathbf{g}, \quad (2)$$

where  $\mathfrak{S} = -p\mathbf{I} + \mathfrak{T}$ ,  $\mathfrak{T} = \eta(\nabla \mathbf{u} + (\nabla \mathbf{u})^T) - \frac{2}{3}\eta(\nabla \cdot \mathbf{u})\mathbf{I}$ , for a Newtonian fluid.

The heat equation is

$$\nabla \cdot \dot{\mathbf{q}} = 0 \quad (3)$$

and the mass species equation is

$$\nabla \cdot \dot{\mathbf{N}}_i = 0, \quad (4)$$

where  $\dot{\mathbf{N}}_i = -D_i \nabla c_i + c_i \mathbf{u}$  and  $\dot{\mathbf{q}} = -k \nabla T + \sum_i h_i \dot{\mathbf{N}}_i$  are fluxes. It should be mentioned that in the above partial differential equations all the physical properties can depend on the temperature and concentration of each component. Normal components of the fluxes and velocities vanish on B1 boundary  $\dot{\mathbf{N}}_{iG} \cdot \mathbf{n} = 0$ ,  $\dot{\mathbf{q}}_G \cdot \mathbf{n} = 0$  and  $\mathbf{u}_G \cdot \mathbf{n} = 0$  as well as the stress  $\mathbf{t} \cdot \mathfrak{S}_G \mathbf{n} = 0$ . On closed isolated boundaries B2 and B6 normal components of the fluxes vanish  $\dot{\mathbf{N}}_{iG} \cdot \mathbf{n} = 0$ ,  $\dot{\mathbf{q}}_G \cdot \mathbf{n} = 0$ , as well as the velocity  $\mathbf{u}_G = \mathbf{0}$  (no-slip condition). Normal components of molar fluxes vanish on closed boundary B8 :  $\dot{\mathbf{N}}_{iL} \cdot \mathbf{n} = 0$ , similarly velocity  $\mathbf{u}_L = \mathbf{0}$  (no-slip condition). Temperature is fixed ( $T_L = T_w$ ). On the inlet open boundary B7 the velocity of liquid is fixed ( $\mathbf{u}_L = \mathbf{u}_{Lin}$ ), where

$$\mathbf{u}_{Lin} = (u_{Lin}, v_{Lin})^T, \quad u_{Lin} = 0, \quad v_{Lin} = \frac{\rho_L g}{4\eta_L} (r^2 - r_2^2 + 2r_1^2 \ln \frac{r_2}{r}), \quad r_1 \leq r \leq r_2 \quad (5)$$

is undisturbed velocity profile of isothermal, gravitational liquid flow along vertical, cylindrical wall. The temperature and the components concentration of the inflow liquid are also fixed ( $T_L = T_{Lin}$ ,  $c_{iL} = c_{iLin}$ ). On the outlet open boundary B5, the normal components vanish: conductivity flux  $-k_L \nabla T_L \cdot \mathbf{n} = 0$ , diffusion flux  $-D_{iL} \nabla c_{iL} \cdot \mathbf{n} = 0$  and viscous stress  $\mathfrak{T}_L \cdot \mathbf{n} = \mathbf{0}$ . On the outflow open boundary B3, the normal components vanish: conductivity flux  $-k_G \nabla T_G \cdot \mathbf{n} = 0$ , diffusion fluxes  $-D_{iG} \nabla c_{iG} \cdot \mathbf{n} = 0$  and viscous stress  $\mathfrak{T}_G \cdot \mathbf{n} = \mathbf{0}$ . Pressure is fixed ( $p_G = p_{Gout}$ ). On the interior boundary B4 the continuity of normal component of molar fluxes  $\dot{\mathbf{N}}_{iL} \cdot \mathbf{n} = \dot{\mathbf{N}}_{iG} \cdot \mathbf{n}$  (principle of mass conservation) as well as thermal energy  $\dot{\mathbf{q}}_L \cdot \mathbf{n} = \dot{\mathbf{q}}_G \cdot \mathbf{n}$  (principle of energy conservation) are valid<sup>4</sup>. The last equation could be transformed into the form  $(k_G \nabla T_G - k_L \nabla T_L) \cdot \mathbf{n} = \sum_i \Delta H_i \dot{\mathbf{N}}_{iL} \cdot \mathbf{n}$ , which shows discontinuity of conduction heat flux on the interface. Existence of the thermodynamic equilibrium state is assumed on the interface. So there is temperature equality  $T_L = T_G$  and the equality of chemical potential, which is described as  $p_G x_{iG} \gamma_{iG} = p_i^{sat} x_{iL} \gamma_{iL}$ . Liquid vaporization causes sudden velocity growth in the direction perpendicular to the surface. Tangential component of the velocity conserves continuity, and because of that kinematic boundary condition is as follows:  $(-\sum_i M_i D_{iL} \nabla c_{iL} + \rho_L \mathbf{u}_L) \cdot \mathbf{n} = (-\sum_i M_i D_{iG} \nabla c_{iG} + \rho_G \mathbf{u}_G) \cdot \mathbf{n}$ ,  $\mathbf{u}_L \cdot \mathbf{t} = \mathbf{u}_G \cdot \mathbf{t}$ . Dynamic boundary condition results from the force balance on the interface<sup>5</sup>  $(\mathfrak{S}_G - \mathfrak{S}_L) \mathbf{n} = \dot{m}_v (\mathbf{u}_G - \mathbf{u}_L) + \sigma(1/R_1 + 1/R_2) \mathbf{n}$ , where  $\dot{m}_v = (-\sum_i M_i D_{iL} \nabla c_{iL} + \rho_L \mathbf{u}_L) \cdot \mathbf{n}$  is mass rate of vaporization. Pressure condition  $p_G = \sum_i p_i^{sat} x_{iL} \gamma_{iL}$  finishes the list of boundary conditions on the gas-liquid interface.

#### 4. Numerical solution

The differential equations have been discretized according to the finite element method<sup>1</sup>. Direct linear system solver – PARDISO was applied. Relative tolerance:  $10^{-6}$  was presupposed. Numerical grid with triangular mesh elements was constructed. Lagrangian quadratic shape functions were used. Spatial (grid) convergence has been examined. Simulations were performed for laboratory thin-layer evaporator with the following dimensions:  $r_2=0.030\text{m}$ ,  $z_1=0.266\text{m}$ ,  $z_2=0.380\text{m}$ ,  $z_3=-0.020\text{m}$ . The evaporator works at steady state. Evaporation of water (1)-propylene glycol (2) solution takes place in the apparatus. The process goes on at  $p_{Gout} = 3333 \text{ Pa}$  (25 mmHg) pressure, with constant wall temperature  $T_w = 364 \text{ K}$ . Liquid is supplied to the evaporator with fixed composition  $x_{1Lin} = 0.1788$  and at boiling point  $T_{Lin} = 334 \text{ K}$ . Five liquid layer thickness  $s = r_2 - r_1$ , i.e. 0.2, 0.3, 0.4, 0.5 i 0.6 mm were considered. The evaporation ratio at these conditions are small and constant value of liquid film thickness along the height of the evaporator was presumed, so the gas-liquid interface is cylindrical surface with constant radius  $r_1$ . The formulas describing the dependences of physical properties of water and propylene glycol on temperature were taken from the literature<sup>6-7</sup>. Similarly the formulas describing the dependences of the mentioned properties on solution composition were taken from the literature<sup>8</sup>. Gas density was calculated from the ideal gas law. Liquid phase activity coefficients were approximated with polynomials based on experimental data published by Gmehling<sup>9</sup>. Gas phase activity coefficients are equal 1. The dependence of diffusion coefficients of water in propylene glycol on temperature and solution viscosity was taken into consideration, applying data published in DIPPR<sup>10</sup>. Diffusion coefficients in gas phase, depending on pressure and temperature were calculated from Fuller formula<sup>8</sup>.

**Table 1.** Basic results

s	$\dot{m}_{Lin}$	$\dot{m}_{Lout}$	$\bar{v}_{Lout}$	$\bar{x}_{1Lout}$	$\bar{T}_{Lout}$	$\dot{m}_{Gout}$	$\bar{v}_{Gout}$	$\bar{x}_{1Gout}$	$\bar{T}_{Gout}$	$\bar{q}_w$	$\gamma_q$
mm	kg/s	kg/s	m/s	-	K	kg/s	m/s	-	K	W/m <sup>2</sup>	-
0.6	4.167E-2	4.163E-2	-0.3731	0.1764	342.94	3.551E-5	0.504	0.9379	334.11	2.332E4	0.0596
0.5	2.591E-2	2.583E-2	-0.2781	0.1713	346.23	8.040E-5	1.116	0.9303	335.58	2.173E4	0.1423
0.4	1.457E-2	1.441E-2	-0.1942	0.1537	350.39	1.602E-4	2.115	0.9097	338.97	1.984E4	0.2968
0.3	6.455E-3	6.196E-3	-0.1117	0.0985	355.89	2.589E-4	3.077	0.8606	344.85	1.669E4	0.5181
0.2	1.814E-3	1.643E-3	-0.0447	0.0251	363.98	1.709E-4	1.714	0.7705	351.85	7.944E3	0.6239

#### 5. Results and discussion

Direct calculation results, obtained with the help of program that solves system of differential equations, are two-dimensional fields of concentration, temperature, pressure and velocity of gas and liquid. Cross-sections in liquid region, that represent four points of z axis are presented in graphs (Fig.2). If the thickness of flowing down liquid layer equals 0.6 mm the changes of water concentration in propylene glycol are small and arise only at the neighbourhood of interface. The liquid layer flows down with high velocity, which overcomes 0.5 m/s on the interface. When we consider thinner and thinner liquid layers the changes of concentration grow and the liquid velocity diminishes. The changes of liquid flowrate along the height are small. Flowing liquid drags gas that is near by liquid surface. On the boundary B4 there is a jump of the radial component of velocity, caused by liquid vaporization. In the graphs the distributions of heat and mass flux densities are presented. Heat flux going through the heated side-wall is higher than the flux going through the interface. The difference, which is used for liquid heating up, is bigger if liquid layer is thick. The heat flux going through the interface is consumed by the process of vaporization. If we observe the interfacial surface along the z axis, from liquid inflow downward, then we can notice that water flux at first goes down, which is caused by a little temperature reduction, after that it grows, which is on the other hand caused by heat inflow to liquid from the hot wall, and in the end the flux of water goes down (for  $s < 0.4 \text{ mm}$ ), which is caused by considerable drop of water concentration in liquid phase. For thinner liquid layers the interfacial temperature grows strongly and the concentration of water in liquid diminishes quickly. In gas phase the changes of concentration and temperature in the evaporator are small. Figure 2 presents streamlines in the domain of gas flow. For  $s=0.6\text{mm}$  the rate of vaporization is small and the velocity of the interface is high, and because of that streamlines go out steeply from interface. One can notice the zone of gas circulation there. For  $s=0.2\text{mm}$  the rate of liquid vaporization at the upper

part of the evaporator is high and the velocity of interfacial surface low, and it causes that the streamlines go out from the interfacial surface at small angles. The results of final calculations, concerning the whole evaporator, are presented in Table 1. It is apparent from this table significant influence of liquid layer thickness on vaporization ratio and thermal efficiency of the process.

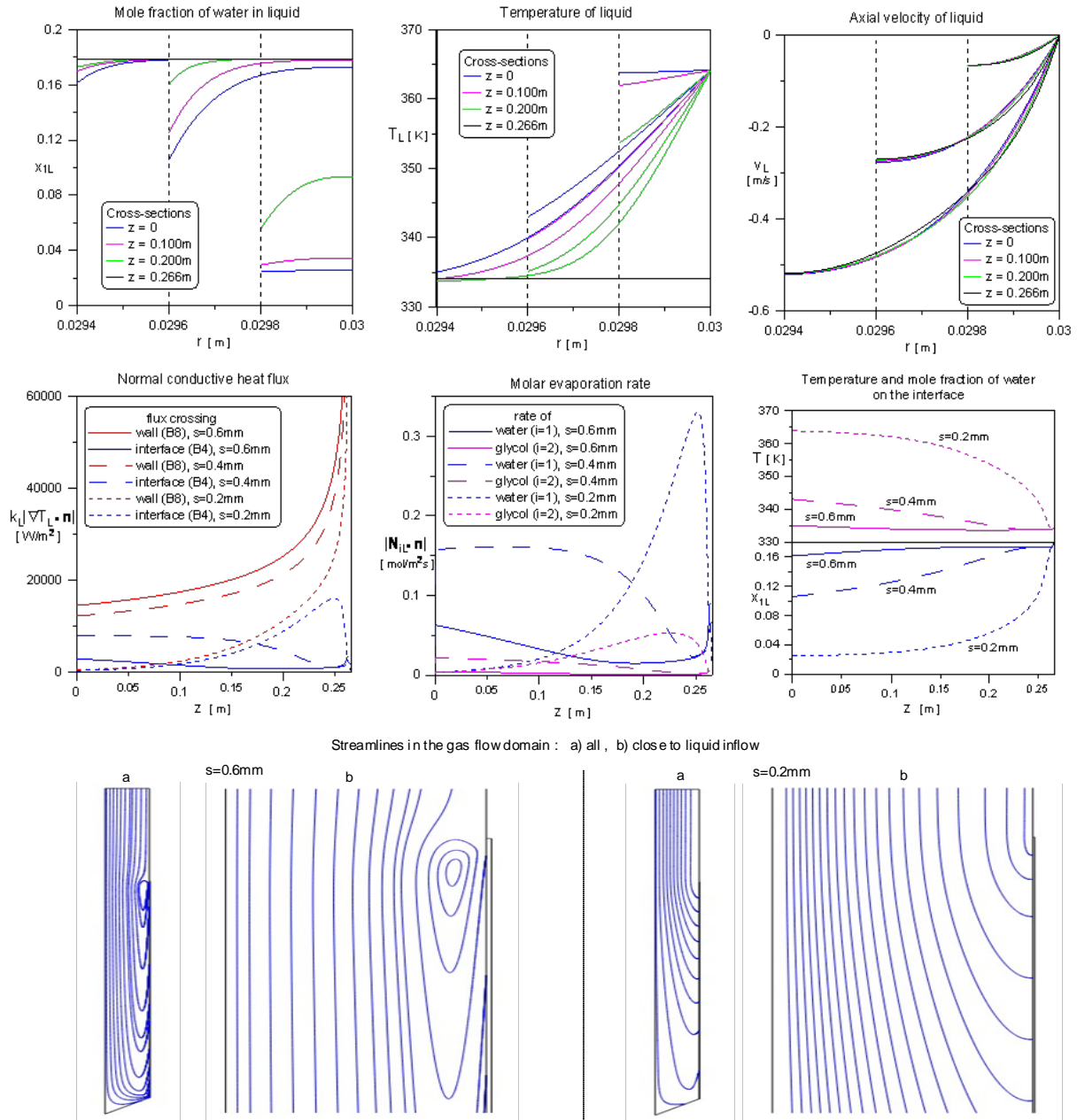


Figure 2. Graphical presentation of CFD simulations.

## 6. Conclusions

Taking into account the results of the proceeded simulations one can notice a concentration gradient in liquid phase at the neighbourhood of the interface. The concentration of the more volatile component on the interface is lower than that in the bulk of liquid at the specified cross-section of the evaporator. As the vapor-liquid equilibrium is established on the interface, it becomes obvious that the theory that takes average liquid concentration at specified cross-section of the thin-layer evaporator (Billet's theory) for determination of gas phase concentration should lead to the wrong results. The

gradient of concentration in liquid phase at specified cross-section of the evaporator is greater for smaller values of liquid layer thickness, so for those cases simplified theory should give greater differences in compare with the experimental results. The gradient of concentration in liquid phase causes also the rise of liquid temperature to the values, which are not expected, applying Billet's theory. This could lead to degradation of heat sensitive components present in liquid phase.

## Nomenclature

$c$  – molar concentration, mol/m<sup>3</sup>,  
 $C_p$  – specific heat capacity at constant pressure, J/kg K ,  
 $D$  – molecular diffusivity, m<sup>2</sup>/s ,  
 $\Delta H$  – enthalpy of vaporization, J/mol ,  
 $\eta$  – dynamic viscosity, Pa s ,  
 $g$  – gravity acceleration, m/s<sup>2</sup>,  
 $\mathbf{g}$  – gravity acceleration vector, m/s<sup>2</sup>,  
 $\gamma$  – activity coefficient,  
 $\gamma_q$  – thermal efficiency (heat flux crossing interface / heat flux crossing heated wall),  
 $h$  – specific enthalpy, J/mol ,  
 $\mathbf{I}$  – unit tensor,  
 $k$  – thermal conductivity, W/m K ,  
 $\dot{m}$  – mass flow rate, kg/s ,  
 $\dot{m}_v$  – mass rate of vaporization, kg/m<sup>2</sup>s ,  
 $M$  – molecular weight, kg/mol,  
 $\mathbf{n}$  – unit normal outward vector,  
 $\dot{\mathbf{N}}$  – total molar flux vector, mol/m<sup>2</sup>s ,  
 $p$  – pressure, Pa ,  
 $\dot{\mathbf{q}}$  – total heat flux vector, W/m<sup>2</sup>,  
 $r$  – radial coordinate, m ,  
 $R_1, R_2$  – radii of curvature, m ,  
 $\rho$  – density, kg/m<sup>3</sup>,  
 $\mathfrak{S}$  – total stress tensor, N/m<sup>2</sup>,  
 $\sigma$  – surface tension, N/m ,  
 $\mathbf{t}$  – unit tangent vector,  
 $T$  – temperature, K ,  
 $\mathfrak{T}$  – viscous stress tensor, N/m<sup>2</sup>,  
 $u$  – radial component of velocity, m/s ,  
 $\mathbf{u}$  – velocity vector, m/s ,  
 $v$  – axial component of velocity, m/s ,  
 $x$  – mole fraction,  
 $z$  – axial coordinate, m ,

### Subscripts:

$i$  – component,  
 $in$  – inflow,  
 $out$  – outflow,  
 $G$  – gas,  
 $L$  – liquid,  
 $w$  – heated wall,

### Superscripts:

$sat$  – saturation,  
 $T$  – transposition,  
 $-$  – average.

### Operators:

$\nabla$  – nabla,  
 $\cdot$  – scalar product.

## References

1. R. Löhner, *Applied CFD Techniques. An Introduction based on Finite Element Methods* (2<sup>nd</sup> ed.), Wiley (2008)
2. J.Dziak, J.Kaplon, L. Krolikowski, L.Ludwig, *Comp.-Aid. Chem. Eng.*, Vol. 26, Elsevier (2009)
3. R. Billet, *CZ-Chemie-Technik*, 3, No.1 (1974)
4. L.G. Leal, *Advanced Transport Phenomena. Fluid Mechanics and Convective Transport Processes*, Cambridge University Press (2007)
5. D. Jamet, *Diffuse interface models in fluid mechanics*, <http://pmc.polytechnique.fr/mp/GDR/docu/Jamet.pdf>
6. C.L. Yaws, *Chemical Properties Handbook*, McGraw-Hill (1999)
7. C.L. Yaws, *Yaws' Handbook of Thermodynamic and Physical Properties of Chemical Compounds*, Knovel (2003)
8. B.E. Poling, J.M. Prausnitz and J.P. O'Connell, *Properties of Gases and Liquids* (5<sup>th</sup> ed.), McGraw-Hill (2001)
9. J. Gmehling, U.Onken and W. Arlt, *Vapor – Liquid Equilibrium Data Collection*, Vol. I, Part 1, Dechema (1990)
10. DIPPR 882 – *Transport Properties and Related Thermodynamic Data of Binary Mixtures. Parts 1 – 4*. By: B.E. Gammon et.al., Design Institute for Physical Property Data / AIChE (1993 – 97).